JOURNAL OF APPLIED PHYSICS VOLUME 85, NUMBER 1 1 JANUARY 1999

Piezoresistive response induced by piezoelectric charges in *n*-type GaAs mesa resistors for application in stress transducers

Y. W. Hsu[a] and S. S. Lu
Department of Electrical Engineering, National Taiwan University, Taipei, Taiwan, Republic of China

P. Z. Chang
Institute of Applied Mechanics, National Taiwan University, Taipei, Taiwan, Republic of China

(Received 27 April 1998; accepted for publication 8 September 1998)

The resistance change due to piezoelectric charge densities in n-GaAs mesa resistors has been studied as a function of surface stress. Those changes are verified by measuring some realized stress transducers with such resistors fabricated on the surface of micromachined thin GaAs membranes or GaInP/GaAs cantilever beams. It is shown here that the surface stresses induced by the deformation of cantilever beams can cause nonuniform stress distributions within the resistors, and the stress gradients consequently yield considerable piezoelectric charge densities that lead to an appreciable resistance change. In addition, this effect of piezoelectric charges is examined from several types of resistors that have a different doping, direction, thickness h, and width-to-thickness ratio L/h. According to those results, optimization of this mechanism is related to the doping and geometrical design of GaAs mesa resistors. In addition to the effect of piezoelectric charges, mobility change can affect the resistance as well. The resistance changes observed from the low doped resistors exhibit an opposite sign for the resistors oriented along $[011]$ and $[01\bar{1}]$ directions. These directional-dependent characteristics confirm that the effect of piezoelectric charges indeed exists in mesa resistors. Fitting the width-dependent sensitivities measured in experiments allows us to estimate each contribution of these two effects. For the $[01\bar{1}]$ oriented resistors with L/h of 10, and n_s of 4.8×10^{11}, the sensitivity of relative resistance change as high as 92.7%/GPa is obtained. Results in this study demonstrate that the resistance change in n-GaAs mesa resistors is attributed to the effects of piezoelectric charges and mobility change. Moreover, GaInP/GaAs material system with its piezoresistive response originated from piezoelectric charges is highly promising in III–V compound semiconductor stress transducers. © *1999 American Institute of Physics.*
[S0021-8979(98)10323-7]

I. INTRODUCTION

As generally known, GaAs electronic circuits have a higher tolerance in high temperature[1–3] and high radiation[4] environments than that in silicon integrated circuits (ICs). Therefore, GaAs based smart sensors have attracted much attention even though silicon based smart sensors have been widely discussed in the field of microelectromechanical system (MEMS).[5–7] From this perspective, GaAs based stress sensors must be developed for applications involving the GaAs monolithic integration of mechanical sensors and signal circuits. The piezoresistive effect due to a directional-dependent modulation of the average mobility in response to a uniaxially applied stress is a well adopted sensing mechanism in silicon based mechanical sensors, but, it is only a very small effect in n-GaAs because of its direct band gap structure.[1] The published values of piezoresistance coefficients π_{11}, π_{12}, and π_{44} for n-GaAs are −2.2%/GPa, −3.8%/GPa, and −2.4%/GPa, respectively.[8] Nevertheless, according to a previous investigation, the nonuniform stress distribution introduced into GaAs can produce piezoelectric charge densities of such magnitude as to shift the GaAs field effect transistors (FETs) characteristics[9] appreciably by modifying the free charge densities originally established due to the doping. This is the underlying notion of the piezoelectric modulated effect, implying that the free charge density of GaAs resistors can be modified by external sources if the piezoelectric charge densities induced in GaAs can be altered by external sources. In 1993, Huang *et al.*[10] first reported the resistance changes due to piezoelectric modulated effect in ion implanted GaAs resistors. That investigation confirmed this mechanism in bulk GaAs by a simple, thick cantilever beam cut directly from a GaAs wafer. However, two dielectric stripes must be deposited beneath the resistor to intensify the stress imparted to the diffused GaAs resistor. For practical applications in micromachined stress transducers, epitaxial techniques [e.g., molecular beam epitaxy, (MBE) or liquid phase epitaxy (LPE)] can offer the appropriate material systems with high etching selectivity to precisely control the geometric thickness. In addition, the fabrication process of mesa resistors is simpler than the diffused resistors. Although the piezoresistive response in p-GaAs mesa resistors, i.e., a mechanism which resembles the one in p-type silicon, has been observed and utilized for pressure sensor by Dehé,[11] the fabrication process of p-type GaAs piezoresistors is not very compatible with the one of conventional n-channel FETs. In this study, we propose a model of

[a]Electronic mail: yuhsu105@ms4.hinet.net

 © 1999 American Institute of Physics

Downloaded 01 Mar 2009 to 140.112.113.225. Redistribution subject to AIP license or copyright; see http://jap.aip.org/jap/copyright.jsp

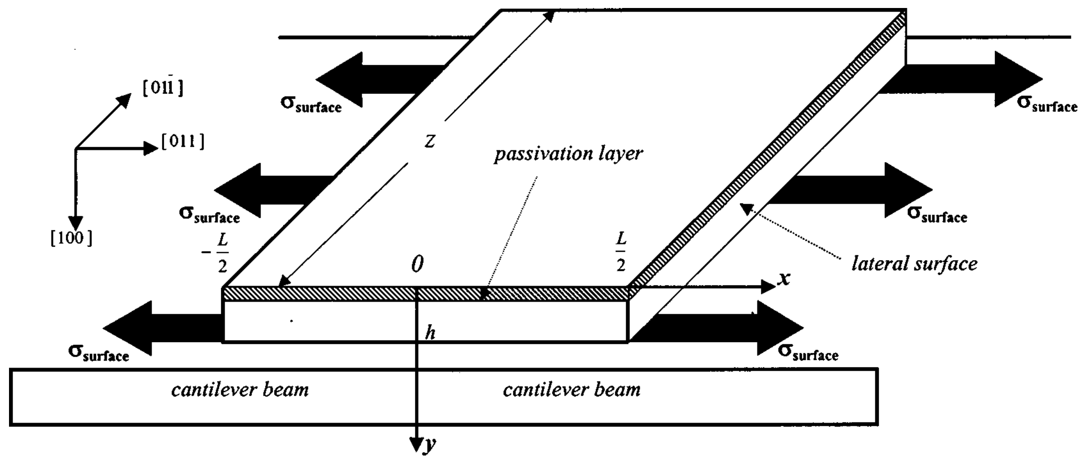

FIG. 1. Schematic diagram of the resistor on cantilever beam and the direction of the elastic tensile surface stress. L is the width of the resistors, and h is the sum of the thickness of resistor and the passivation layer.

the resistance change due to piezoelectric modulated effect in n-GaAs mesa resistors. The feasibility of applying the proposed model in stress and force transducers is experimentally investigated as well.

The stress distribution within mesa resistors differs from that in diffused resistors in previous literature.[9,10] By following the method of Aleck,[12] a two-dimensional nonuniform stress distribution induced by the surface stress could be calculated. By doing so, the piezoelectric charge densities can be numerically determined. As the piezoelectric charges modify the linear charge density of resistors, the resistance change due to the piezoelectric charges is eventually determined as a function of the surface stress. Notably, all of the resistors are passivated with a 50 nm GaInP thin film so that the term of h is the sum of the thickness of resistor layer and passivation layer. In this study, we examine the piezoresistive response, a composite effect attributed to piezoelectric charges and mobility change, by applying it as the sensing mechanism of pressure sensors and accelerometer in which the resistors are fabricated on the thin GaAs membranes and GaInP/GaAs cantilever beams, respectively. Modifying the doping, direction, and L/h ratio of the resistors allows us to optimize the resistance change due to piezoelectric modulated effect in n-GaAs mesa resistors.

The rest of this article is organized as follows. Section II presents the model analysis of the resistance change due to the piezoelectric charge densities in GaAs mesa resistors. Section III describes the experiment details and results. Next, Sec. IV thoroughly discusses the results in this study and, finally, conclusions are made in Sec. V.

II. MODEL ANALYSIS

A. Stress distributions in resistors

As the surface stress acts on the clamped surface of mesa resistors, Fig. 1 schematically depicts the resistor on cantilever beam and the direction of elastic tensile surface stress. For the situation in which the length Z of resistor is markedly larger than the width L of resistors, the stress distribution is considered to be two dimensional[12] so that the components σ_{xz} and σ_{yz} of the stress tensor are set to zero. Stress distribution for this geometry has been estimated[13] by assuming that (a) the GaAs is elastically isotropic and (b) the Poisson's ratio of GaInP is the same as GaAs. For the coordinate system illustrated in Fig. 1, the nonzero components of the stress tensor are of the following form:

$$\begin{aligned}
\frac{\sigma_{xx}}{\sigma_{\text{surface}}} &= 1 - \sum_{i=1}^{3} \sum_{j=1}^{6} A_{i,j} \eta^{i-1} \cosh(\lambda_j \xi), \\
\frac{\sigma_{xy}}{\sigma_{\text{surface}}} &= \sum_{i=1}^{3} \sum_{j=1}^{6} A_{i,j} \frac{\eta^{i}}{i} \lambda_j \sinh(\lambda_j \xi), \qquad (1) \\
\frac{\sigma_{yy}}{\sigma_{\text{surface}}} &= -\sum_{i=1}^{3} \sum_{j=1}^{6} A_{i,j} \frac{\eta^{i+1}}{i(i+1)} \lambda_j^2 \cosh(\lambda_j \xi),
\end{aligned}$$

TABLE I. Calculated results of coefficients λ_j, $A_{2,j}/A_{1,j}$, and $A_{3,j}/A_{1,j}$ for the GaAs Poisson's ratio of 0.31.

j	λ_j	$A_{2,j}/A_{1,j}$	$A_{3,j}/A_{1,j}$
1	-0.968132	-0.171275	-0.721211
2	$-2.57248+1.38623j$	$-4.26023-0.465977j$	$3.11523+0.343618j$
3	$-2.57248-1.38623j$	$-4.26023+0.465977j$	$3.11523-0.343618j$
4	$-6.49648+2.8869j$	$-7.22432-0.344769j$	$8.29658+0.888306j$
5	$-6.49648-2.8869j$	$-7.22432+0.344769j$	$8.29658-0.888306j$
6	-22.1118	-9.26131	13.3017

Downloaded 01 Mar 2009 to 140.112.113.225. Redistribution subject to AIP license or copyright; see http://jap.aip.org/jap/copyright.jsp

where $\sigma_{\mathrm{surface}}$ is the surface stress at the clamped surface; $\xi(\xi=x/h)$ and $\eta(\eta=y/h)$ are normalized coordinate variables; $A_{i,j}$'s are undetermined coefficients dependent on the ratio of $L/2h$ and Poisson's ratio v; and λ_j's are undetermined coefficients dependent on v only. The sign of $\sigma_{\mathrm{surface}}$ is positive as the resistor is forced to expand, whereas the sign of $\sigma_{\mathrm{surface}}$ is negative as the resistor is forced compression. The solution of Eq. (1) involves finding the condition that a symmetrical determinant below vanishes[12]

$$\begin{vmatrix} 2-\left(\frac{4}{3}+2v\right)\lambda^2+\frac{1}{10}\lambda^4 & 1-\left(\frac{1}{2}+\frac{5}{6}v\right)\lambda^2+\frac{1}{36}\lambda^4 & \frac{2}{3}-\left(\frac{4}{15}+\frac{1}{2}v\right)\lambda^2+\frac{1}{84}\lambda^4 \\ 1-\left(\frac{1}{2}+\frac{5}{6}v\right)\lambda^2+\frac{1}{36}\lambda^4 & \frac{2}{3}-\left(\frac{1}{5}+\frac{1}{3}v\right)\lambda^2+\frac{1}{126}\lambda^4 & \frac{1}{2}-\left(\frac{1}{9}+\frac{7}{36}v\right)\lambda^2+\frac{1}{288}\lambda^4 \\ \frac{2}{3}-\left(\frac{4}{15}+\frac{1}{2}v\right)\lambda^2+\frac{1}{84}\lambda^4 & \frac{1}{2}-\left(\frac{1}{9}+\frac{7}{36}v\right)\lambda^2+\frac{1}{288}\lambda^4 & \frac{2}{5}-\left(\frac{4}{63}+\frac{1}{9}v\right)\lambda^2+\frac{1}{648}\lambda^4 \end{vmatrix}=|\Delta|=0. \quad (2)$$

Associated with each root λ_j, a unique relation exists between the $A_{1,j}$, $A_{2,j}$, and $A_{3,j}$ of Eq. (1) to satisfy the condition of $[\Delta]\times[A_{1,j}A_{2,j}A_{3,j}]^T=0$. By using the GaAs Poisson's ratio v of 0.31,[14] the values for the complex constant λ_j, complex ratios $A_{2,j}/A_{1,j}$ as well as $A_{3,j}/A_{1,j}$ have been evaluated and are listed in Table I. By taking account of $L/2h$, the six $A_{1,j}$'s can be determined from the boundary conditions ($\xi=\pm L/2h$: $\sigma_{xx}=0$ and $\sigma_{xy}=0$) by solving a system of six linear equations. Table II lists the calculated values of the corresponding coefficients $A_{1,j}$'s for the two representative examples of $L/2h=5$ and $L/2h=46$.

B. Piezoelectric charge densities in resistors

GaAs is a noncentrosymmetric crystal and has nonzero components of the piezoelectric tensors. For the coordinate system shown in Fig. 1, the components of the piezoelectrically induced polarization vector $[\mathbf{P}]$ are

$$[\mathbf{P}]=\begin{bmatrix} P_x \\ P_y \\ P_z \end{bmatrix}=\begin{bmatrix} d_{14}\sigma_{xy} \\ -\frac{d_{14}}{2}(\sigma_{zz}-\sigma_{xx}) \\ -d_{14}\sigma_{yz} \end{bmatrix}, \quad (3)$$

where $d_{14}=2.6\times10^{-17}$ C/dyn=162.5 electron/dyn.[15,16] If the piezoelectric charge densities $\rho_{\mathrm{PZ}}(x,y)$ are given by $\rho_{\mathrm{PZ}}(x,y)=\nabla\cdot[\mathbf{P}]$, with the assistance of momentum balance equations ($\partial\sigma_{xx}/\partial x=-\partial\sigma_{xy}/\partial y$, $\partial\sigma_{yy}/\partial y=-\partial\sigma_{xy}/\partial x$, and $\sigma_{zz}=v\sigma_{xx}+v\sigma_{yy}$), the piezoelectric charge densities in mesa resistors can thus be found to be

$$\rho_{\mathrm{PZ}}(x,y)=-d_{14}\frac{\partial}{\partial y}\left[\left(1+\frac{v}{2}\right)\sigma_{yy}-\frac{1}{2}(1-v)\sigma_{xx}\right]. \quad (4)$$

As the mesa resistors are strained by the tensile surface stress of 10^8 dyn/cm^2, Figs. 2(a) and 2(b) display the calculated distributions of $\rho_{\mathrm{PZ}}(x,y)/q$ for $L/2h=5$ and $L/2h=46$, respectively. These figures also illustrate the phenomenon in which the distributions of $\rho_{\mathrm{PZ}}(x,y)/q$ have a sharper variation near the lateral surfaces. This is because the stress distribution varies rapidly near lateral surfaces. Figures 2(c) and 2(d) illustrate the logarithmic plots of $\rho_{\mathrm{PZ}}(x,y)/q$ over the range $0\leqslant x/h\leqslant L/2h-1$ and $0\leqslant y/h\leqslant1$, where the lowest value of $\rho_{\mathrm{PZ}}(x,y)/q$ exists at the central point on top surface. For $L/2h=5$, although the lowest value of 10^{12} charges/cm^3 is obtained, the corresponding position with the value of 10^{12} charges/cm^3 is located at the position $x/h\rightarrow41$ for $L/2h=46$.

C. Effects on resistance change

The piezoelectric charges can be detected because they are fixed and thereby capable of altering the conductance in GaAs. Muller *et al.* first proposed this concept in CdS.[17] The depletion regions which originated from the surface states exist in the vicinity of the boundary surfaces so that the piezoelectric charges may simultaneously change the resistance through two mechanisms. The piezoelectric charges in depletion region are uncompensated, and they modify the width of depletion region. On the other hand, the piezoelec-

TABLE II. Calculated $A_{1,j}$'s for $L/2h$ of 5, and 46.

j	$A_{1,j}$ for $L/2h=5$	$A_{1,j}$ for $L/2h=46$
1	$-3.94454\times10^{-18}+3.71569\times10^{-33}$	9.8216×10^{-20}
2	$6.07427\times10^{-6}-3.25861\times10^{-6}\,j$	$-4.69543\times10^{-52}+2.20719\times10^{-52}\,j$
3	$6.07427\times10^{-6}+3.25861\times10^{-6}\,j$	$-4.69543\times10^{-52}-2.20719\times10^{-52}\,j$
4	$5.51104\times10^{-16}-7.36415\times10^{-15}\,j$	$9.51265\times10^{-131}-4.55439\times10^{-131}\,j$
5	$5.51104\times10^{-16}+7.36415\times10^{-15}\,j$	$9.51265\times10^{-131}+4.55439\times10^{-131}\,j$
6	$2.50957\times10^{-49}+9.42287\times10^{-64}\,j$	0

Downloaded 01 Mar 2009 to 140.112.113.225. Redistribution subject to AIP license or copyright; see http://jap.aip.org/jap/copyright.jsp

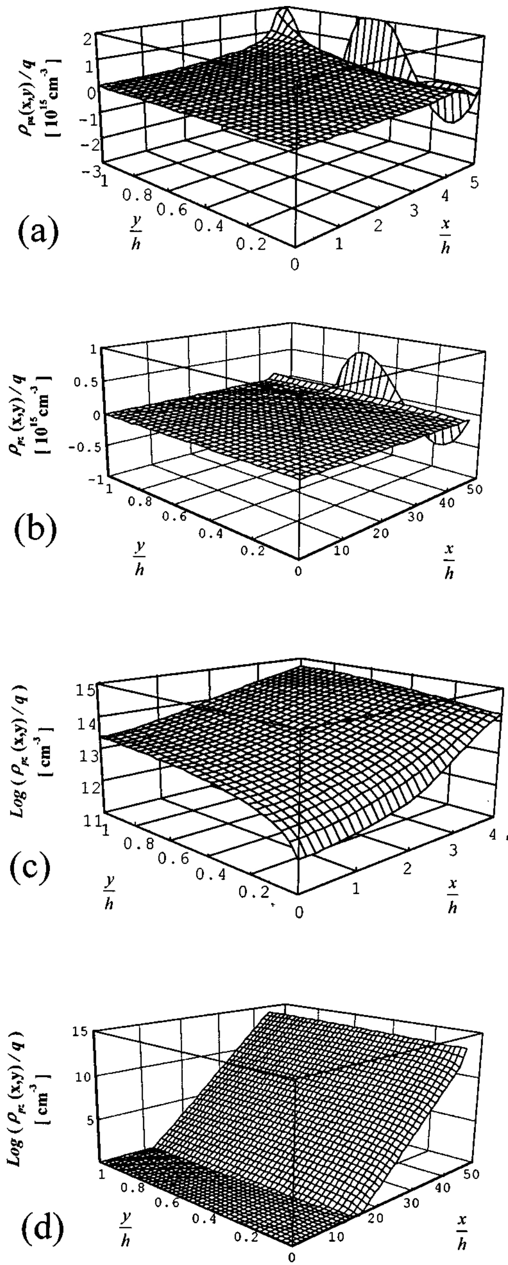

FIG. 2. Calculated piezoelectric charge densities for the resistors of (a) $L/2h=5$, (b) $L/2h=46$ strained by the tensile surface stress of 10^8 dyn/cm^2. Logarithmic plot of piezoelectric charge density over the range $0\leqslant x/h \leqslant L/2h-1$ and $0\leqslant y/h\leqslant 1$ for the resistors with (c) $L/2h=5$, (d) $L/2h=46$.

tric charge densities in the channel combine with the charge densities established due to impurity doping, thereby altering the free carrier concentration in the channel.

For the resistors without a strain, the conductance G_0 is given by

$$G_0=\frac{q\mu_0}{Z}\int_{-L/2+\varpi}^{L/2-\varpi}\int_{t_{\min,0}}^{t_{\max,0}}N_D dy dx=\frac{2q\mu_0 w_0 n_s}{Z}, \tag{5}$$

where q is the magnitude of the electronic charge, Z is the length of the resistors, μ is electron mobility, ϖ is the lateral depletion width, $t_{\min,0}$ is the depth of the top depletion region, $t_{\max,0}$ is the depth of the bottom depletion region, N_D is the uniform doping in resistors, and n_s is the sheet charge density. The subscripts 0 denote a situation in which the resistors are not strained. For the resistors with strain, we neglect the effects associated with possible shifts of the surface states and further assume that the stress independent densities characterize the surface states. Because the piezoelectric charge densities in the region $x/h\leqslant|L/2h-5|$ are much smaller than those in the region $x/h\geqslant|L/2h-5|$, as shown in Figs. 2(c) and 2(d), the conductance changes in the regions $x/h\geqslant|L/2h-5|$ can be considered as having originated from the effect of piezoelectric charges. In addition, the resistance changes in the regions $x/h\leqslant|L/2h-5|$ appear to be attributed to the effect of mobility change. Thus, G_0 is the sum of G_{PE}, which is the conductance in the region $x/h\geqslant|L/2h-5|$, and G_μ, which is the conductance in the region $x/h\leqslant|L/2h-5|$. The conductance change ΔG can be expressed as

$$\Delta G=\frac{2\mu_0}{Z}\int_{t_{\min,0}-\Delta t_{\min}}^{t_{\max,0}+\Delta t_{\max}}\int_{L/2-5h}^{w_0}\rho_{\mathrm{PZ}}(x,y)dxdy + \frac{\mu_0 q N_D(2w_0+10h-L)}{Z}\times\Delta t+\frac{qn_s(L-10h)}{Z}\times\Delta\mu=\Delta G_{\mathrm{PE}}+\Delta G_\mu. \tag{6}$$

where $\Delta\mu$ is the mobility change in response to uniaxial stress, $\Delta t(\Delta t=\Delta t_{\min}+\Delta t_{\max})$ is the vertical dimension variation due to piezoelectric charges in depletion region, ΔG_{PE} is the conductance change due to the piezoelectric charges, and ΔG_μ is the conductance change due to the mobility change. Herein, the lateral dimension variation of channel is neglected because L is markedly larger than h in our study. The vertical dimension variations of channel may be determined from perturbative solutions to the one-dimensional Poisson equation in y direction. In Eq. (6), ΔG_{PE} can be estimated assuming that the vertical dimension variation of channel is uniform in the x direction and it is the sum of top depletion variation $\Delta t_{\min}$ and bottom depletion variation $\Delta t_{\max}$, where the value of $\Delta t_{\min}$ and $\Delta t_{\max}$ are given by the computed result for $x/h=\pm(L-5h)/2h$. The fractional resistance change $\Delta R/R_0$ can be expressed as

$$\frac{\Delta R}{R_0}\approx-\frac{\Delta G}{G_0}=-\frac{\Delta G_\mu+\Delta G_{\mathrm{PE}}}{G_\mu+G_{\mathrm{PE}}}. \tag{7}$$

For the [011] oriented resistors, the piezoelectric polarization vector has the opposite sign in Eq. (3) so that $\rho_{\mathrm{PZ}}(x,y)$ given by Eq. (4) also have the opposite sign to one of the resistors oriented along $[01\bar{1}]$. This finding indicates that the resistance change due to piezoelectric charges is directional dependent.

III. EXPERIMENT DETAILS

Three layer structures have been grown on (100) semi-insulating (SI) GaAs substrates for our piezoresistivity studies. The first layer structure designed for pressure sensor, referred to herein as sample A, was grown on SI substrate by gas source molecular beam epitaxy (GSMBE) as follows. A 600 nm GaAs n ($\sim 3.4\times10^{16}$ cm^{-3}, Si doped) resistor layer

Downloaded 01 Mar 2009 to 140.112.113.225. Redistribution subject to AIP license or copyright; see http://jap.aip.org/jap/copyright.jsp

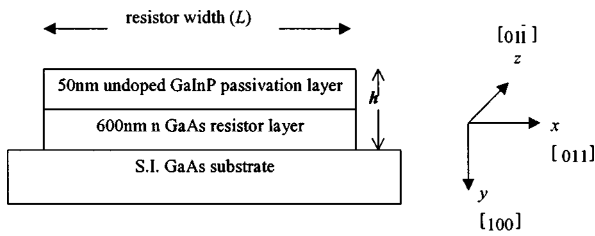

FIG. 3. Illustration diagram of the layer structures of sample A. The width of the $[01\bar{1}]$ oriented resistors fabricated on sample A were designed to be 14, 22, 40, and 60 μm. The corresponding ratios of $L/2h$ with the width of resistors are 11, 17, 30, and 46.

was initially grown and, then, a 50 nm GaInP passivation layer was grown. As the GaAs resistors were passivated by a thin GaInP layer, the interface charge density on the interface of GaInP/GaAs lowers the band bending in GaAs.[18] Four types of $[01\bar{1}]$ oriented resistors with different ratio of $L/2h$ were fabricated on sample A. Figure 3 schematically depicts the layer structures of sample A, where the ratio of $L/2h$ for the resistors on sample A was designed to be 11, 17, 30, and 46, respectively. The second layer structure designed for pressure sensor, which we call sample B, was different from the sample A by replacing the resistor layer with a 300 nm GaAs n ($\sim 4.9\times 10^{17}$ cm^{-3}, Si doped) resistor layer. The resistors on sample B were oriented along [011] direction and the ratio of $L/2h$ were designed to be 43, 57, and 86, respectively. Figure 4 displays a finished pressure-sensor structure, where the sizes of the proof mass and the membrane thickness were designed to be 2000 μm$\times$2000 μm$\times$400 μm and 60 μm, respectively. Furthermore, we also fabricated the [011] oriented resistor with $L/2h = 46$ on sample A; however, the membrane thickness was reduced to 6 μm. The thickness of membranes was controlled by a depth-calibration hole that has been initially etched from the front side and as deep as the required membrane thickness.

The third layer structure designed for accelerometer, referred to herein as sample C, was grown as follows. A 200 nm GaInP undoped etching stop layer was initially grown on a (100) SI. GaAs substrate, followed by a 2 μm GaAs undoped layer as the main structure layer of two beams. Next, a 400 nm GaInP undoped insulating layer was grown on top of the structure layer. Finally, a 150 nm GaAs n ($\sim 5.7 \times 10^{16}$ cm^{-3}, Si doped) resistor layer with a 50 nm GaInP passivation layer was grown. The resistors of $L/2h = 5$ realized on sample C were oriented along $[01\bar{1}]$ direction. Figure 5 depicts the accelerometer with its layer and geometric dimensional structure, where the sizes of the proof mass and the two beams were designed to be 1000 μm $\times$1000 μm$\times$400 μm and 600 μm$\times$500 μm$\times$2.6 μm, respectively. The two beams composed of GaInP/GaAs/GaInP multiple layers (total 2.6 μm) were designed to be so thin that they could offer a higher induced surface stress and, hence, a higher sensitivity in responding to external acceleration. For exact thickness control, adopting a material system with a high etching selectivity is indispensable. Therefore, GaInP/GaAs material system was selected herein owing to its high etching selectivity between GaInP and GaAs.[19–21] During the fabrication, H_2SO_4:H_2O_2:H_2O solution was used to etch GaAs while HCl:H_2O solution was used to etch GaInP. Figure 6 illustrates an example of high etching selectivity between GaInP and GaAs, where the thickness of the GaInP microbridges was 400 nm and the gap under the bridges was 10 μm. For the metallizations of the ohmic contacts and electrodes, Au/Ge/Ni alloy and the Cr/Au were evaporated, respectively.

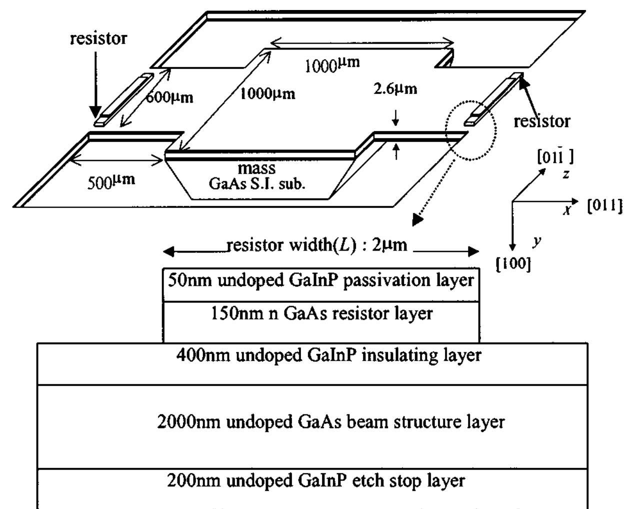

FIG. 5. Schematic diagram of the layer structures of the sample C and the geometric dimensional structure designed for accelerometer. The width of the $[01\bar{1}]$ oriented resistors of $L/2h = 5$ and the thickness of the cantilever beams are designed to be 2 and 2.6 μm, respectively.

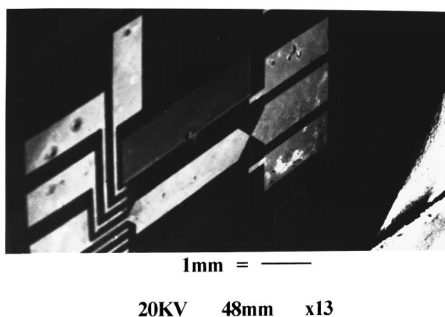

FIG. 4. Scanning electron micrograph of a finished pressure sensor.

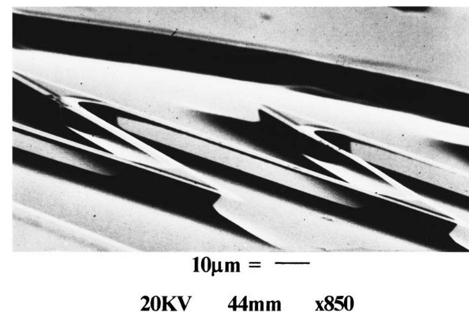

FIG. 6. Scanning electron microscopy (SEM) photograph of an illustrative example of high etching selectivity between GaInP and GaAs. The thickness of the GaInP microbridges is 400 nm.

Downloaded 01 Mar 2009 to 140.112.113.225. Redistribution subject to AIP license or copyright; see http://jap.aip.org/jap/copyright.jsp

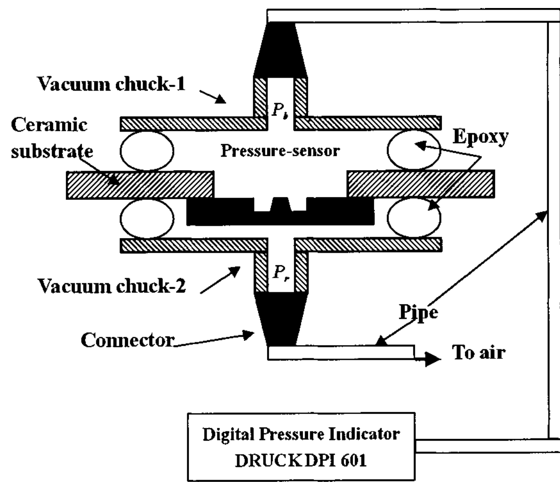

FIG. 7. The setup of test apparatus for the pressure sensors. As the chuck 1 is connected to the pressure indicator, the chuck 2 is alternately connected to ambient pressure. P_b denotes the pressure on the backside and P_r denotes the pressure on the front side. The pressure difference (P) across the membrane is given by $P=P_b-P_r$.

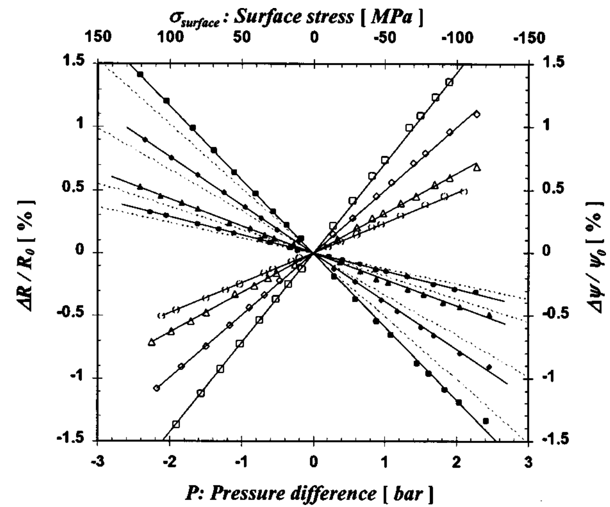

FIG. 8. The characteristics of fractional resistance change (open symbols) against the pressure difference and the corresponding $\Delta\psi/\psi_0$ (solid symbols) vs surface stress for the $[01\bar{1}]$ oriented resistors with $L/2h$ of 11 (□, ■), 17 (◇, ◆), 30 (△, ▲), and 46 (○, ●) on sample A. The dashed lines represent the theoretical values.

The electrodes on the finished pressure sensors were wire bonded with the ceramic substrates and, then, pressure sensors were attached on the ceramic substrates with the epoxy. The test of the pressure sensors fabricated on sample B was performed by a static method. Figure 7 schematically depicts a simple test apparatus. For this purpose, two vacuum chucks were used. The chuck 1 was connected to a pressure indicator of DRUCK DPI 601 which offers the positive pressure and pressure control. If the pressure on the backside of the sample was denoted by P_b, the pressure on the front side (P_r) was reduced to produce a pressure difference $P=P_b-P_r$ across the membranes. For the condition shown in Fig. 7, P_r is the ambient pressure and is assumed to remain constant at 1 atm so that the pressure difference is positive. The condition of negative pressure difference was obtained by switching the pressure indicator from chuck 1 to chuck 2. Figures 8 and 9 plot the characteristics of the experimentally observed $\Delta R/R_0$ vs pressure difference P for the resistors on samples A and B, respectively, where the resistors were strained by the compressive surface stress for $P>0$ and strained by the tensile surface stress for $P<0$. Figure 10 displays the measurement of the resistor fabricated on the thin membrane of 6 μm, where the sample was observed over the pressure range 0 to -0.4 bar.

Herein, the test of the accelerometers fabricated on sample C was performed by a dynamic method. The finished accelerometers were fixed on a vibration excitor of BK type 4809 for testing and a commercial accelerometer of PCB301 A03 was put on the same excitor to readout the acceleration. Meanwhile, a periodic signal generated by a function generator of HP-3245A was amplified through a YAMAHA MX-830 power amplifier to push the excitor. A constant current was sent into the resistors of the fabricated accelerometer to offer the bias. The periodic terminal voltages measured by the dynamic signal analyzer of HP-35665A allowed us to determine the periodic resistance change modulated by the acceleration. Figure 11 presents the measurements of $\Delta R/R_0$ against periodic acceleration (a), where the resistor was strained by compressive surface stress for a and the resistors were strained by the tensile surface stress for a. The resistance changes measured from the resistors upon which the compressive surface stresses act have an opposite sign to those observed from the resistors upon which the tensile surface stresses act.

IV. DISCUSSION

Since the resistance affected by the mobility change are assumed to be of equal value for the resistors oriented along $[011]$ and $[01\bar{1}]$ directions, the resistance changes due to mobility change show no directional dependence. According to Figs. 8 and 10, the resistance changes measured from the $[011]$ and $[01\bar{1}]$ oriented resistors on sample A are of oppo-

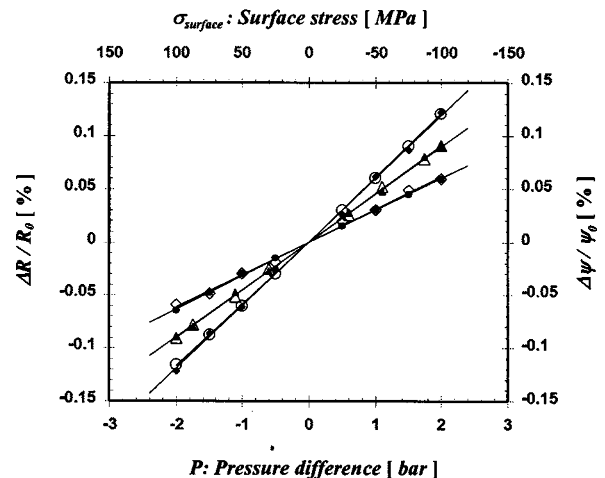

FIG. 9. Relative change of resistance (open symbols) vs the pressure difference and the corresponding $\Delta\psi/\psi_0$ (solid symbols) vs surface stress for the $[011]$ oriented resistors with $L/2h$ of 43 (◇, ◆), 57 (△, ▲), and 86 (○, ●) on sample B.

Downloaded 01 Mar 2009 to 140.112.113.225. Redistribution subject to AIP license or copyright; see http://jap.aip.org/jap/copyright.jsp

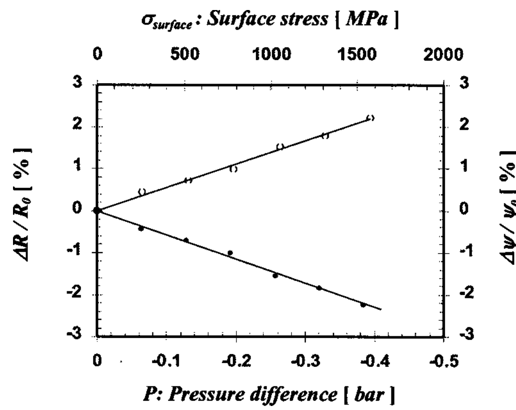

FIG. 10. The measurement of fractional resistance change (open symbols) against the pressure difference and the corresponding $\Delta\psi/\psi_0$ (solid symbols) vs surface stress for the [011] oriented resistors with $L/2h$ of 46 (○, ●) on sample A. This resistor is fabricated on the membrane of 6 μm.

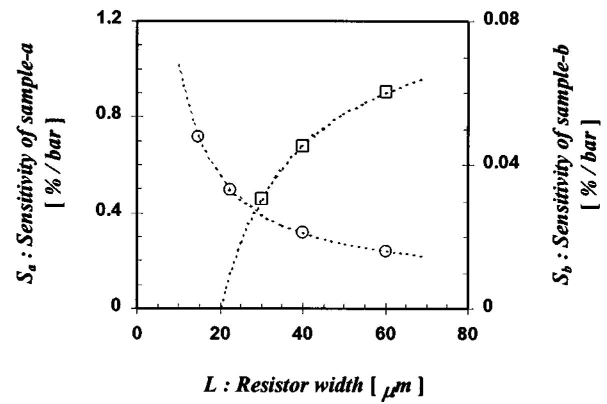

FIG. 12. Sensitivity vs resistor width for the resistors fabricated on samples A and B. S_a (○) denotes the sensitivity measured from the resistors on sample A, whereas, S_b (□) denotes the sensitivity measured from the resistors on sample B. The dashed lines represent the fitted curves. The term of $k\pi_t$ can be extracted by fitting these points with Eq. (8). The dashed lines represent the fitted results.

site sign. Importantly, this finding demonstrates that the resistance changes due to directional-dependent piezoelectric effect definitely exist in mesa resistors. In addition, the piezoelectric modulated effect dominates the resistance change for those resistors fabricated on the sample A. This result confirms the presence of a reliable mechanism of resistance change due to piezoelectric modulated effect in mesa resistors. To distinguish the effect of mobility change from the effect of piezoelectric charges, a simple model is proposed herein and further used to approximately estimate the resistance change resulted from the piezoelectric modulated effect.

For the wide resistors ($L/2h \geqslant 5$), the stress distribution can be divided into two parts: a uniform part that is valid for the central region of the plate (i.e., $x \leqslant |(L-10h)/2|$) and a nonuniform term for the parts in the vicinity of the lateral edges (i.e., $x \geqslant |(L-10h)/2|$). This implies that the effect of piezoelectric charges exists primarily in the region $x \geqslant |(L-10h)/2|$. In line with this assumption, the mesa resistors can be divided into two parts: a mobility-change-dependent resistor with conductance G_μ and a piezoelectric modulated resistor with conductance G_{PE}, where the ratio of G_{PE}/G_μ is $10h/(L-10h)$. Thus, the relative resistance changes in Eq. (7) can be expressed as

$$\frac{\Delta R}{R_0} \approx -\frac{\Delta G_\mu}{G_\mu}\left(\frac{L-10h}{L}\right) - \frac{\Delta G_{\mathrm{PE}}}{G_{\mathrm{PE}}}\left(\frac{10h}{L}\right) = kP\pi_t - \frac{\Delta\psi}{\psi_0}, \tag{8}$$

where k is a transformation factor, P is the pressure difference, π, is the transverse piezoresistance coefficient for GaAs, $\Delta\psi$ is change of linear charge density, and ψ_0 is linear charge density of the channel.

If the relative changes of resistance which originated from the mobility change are assumed to be equal value for those resistors in our experiments, the relative changes of linear charge density can be experimentally extracted for different resistors according to Eq. (8). Figure 12 plots the sensitivities (S), $S = \partial(\Delta R/R_0)/\partial P$, measured from the resistors fabricated on samples A and B, as a function of resistor width. By fitting these points with Eq. (8), the corresponding values of $k\pi_t$ and $\partial(\Delta G_{\mathrm{PE}}/G_{\mathrm{PE}})\partial p$ for sample A have been extracted to be 8.66×10^{-4} and -1.425×10^{-2} bar^{-1}, respectively. On the other hand, the $k\pi_t$ of 9×10^{-4} bar^{-1} and $\partial(\Delta G_{\mathrm{PE}}/G_{\mathrm{PE}})/\partial p$ of 5.13×10^{-3} bar^{-1} were obtained for sample B. By using the values of piezoresistance coefficients reported by Sager,[8] the numerical value of π_t can be estimated by $\pi_t = (\pi_{11}+\pi_{12}-\pi_{44})/2$ to be -1.8%/GPa. According to these results, the transformation factor k of -49 MPa/bar was determined.

For the dimensional parameters of pressure-sensor and accelerometer structures adopted herein, the corresponding surface stress with the external force (pressure or acceleration) has been estimated by the commercial finite element software ANSYS. The $\sigma_{\mathrm{surface}}$ induced by the deformation of the membrane can be expressed as $\sigma_{\mathrm{surface}} = -3.9\times10^{10}p$ dyn/cm^2 (where P is in unit of bar) for the membrane thickness of 6 μm, and the corresponding value of transformation factor is -3.9 GPa/bar. As the terms of k and π_t have been determined, the relative change of linear charge density can be extracted as well. Figures 8–10 illustrate the

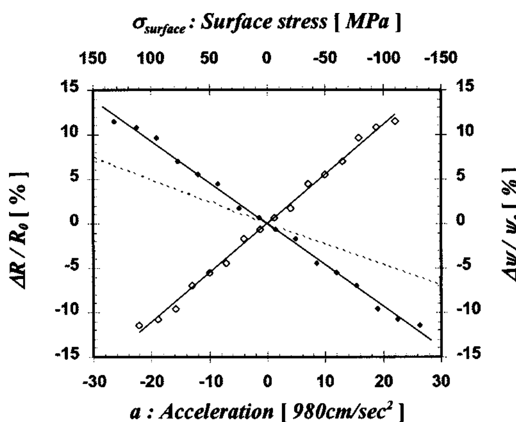

FIG. 11. The characteristics of fractional resistance change (open symbols) vs acceleration and the $\Delta\psi/\psi_0$ (solid symbols) vs surface stress for the $[01\bar{1}]$ oriented resistors with $L/2h$ of 5 (◇, ◆) on sample C. The dashed lines represent the theoretical predictions.

Downloaded 01 Mar 2009 to 140.112.113.225. Redistribution subject to AIP license or copyright; see http://jap.aip.org/jap/copyright.jsp

relative changes of linear charge density against the surface stress for those resistors on samples A and B. Interestingly, the effect of mobility change dominates the resistance change for those resistors fabricated on sample B. Such an effect is attributed to the reduction of $\Delta\psi/\psi_0$. On the other hand, the numerical value of $\sigma_{\mathrm{surface}}$ at the location where the resistors were located is evaluated to be $\sim -6.17 \times 10^7$ a dyn/cm^2, where a is in unit of 980 cm/s^2. For the resistors with $L/2h=5$ on sample C, the resistance changes are considered to be attributed only to the effect of piezoelectric charges. Figure 11 displays the characteristics of $\Delta\psi/\psi_0$ vs surface stress for sample C, where the sensitivity of $\Delta\psi/\psi_0$ of 92.7%/GPa was obtained. This value is comparable to the piezoresistance coefficients of silicon.

In the case of $[01\bar{1}]$ oriented sample A, the corresponding lateral surface band bending of 0.62 eV, ϖ of 162.3 nm, $t_{\mathrm{min},0}$ of 143.9 nm, and $t_{\mathrm{max},0}$ of 487.7 nm are determined. For $\sigma_{\mathrm{surface}}=10^9$ dyn/cm^2, the corresponding Δt of 4.5 nm, and $\Delta\psi$ of 2.736×10^{-12} C/cm have been obtained. The deviation between the measured and predicted $\Delta\psi/\psi_0$ could be attributed to the error of the estimation of Δt, the over simplified estimation of $k\pi_t$, and neglect of the lateral depletion variation. In fact, the distribution of piezoelectric charges in depletion region was two dimensional so that the dimensional variation of channel in the strained resistors was not uniform. To solve the actual dimensional variation of the channel, a two-dimensional Poisson equation must be utilized.

Considerations involving the geometric design and impurity doping are important and flexible for the application in stress or force transducers. For constant surface depletion, ψ_0 is related and proportional to the L, N_D, and the thickness of resistor layer so that these three terms make a simple design rule for further applications of a thin film piezoelectric modulated resistor. Increasing the relative change of linear charge density depends on narrowing down the width of the resistors (i.e., lower the ratio of $L/2h$) and lowering the impurity doping. This phenomenon has been experimentally illustrated by comparing the results observed from samples B and C.

V. CONCLUSIONS

This study presents a novel model of the resistance change due to piezoelectric modulated effect in n-GaAs mesa resistors. Measurements of some realized transducers confirm the proposed model's effectiveness. Measurement results indicate that the piezoresistive response in GaAs mesa resistors leads to the effects of piezoelectric charge densities and mobility change in response to the external surface stress. The doping and the geometric designs of the resistors can markedly influence the fractional change of linear charge density due to the effect of piezoelectric charges, thereby offering some flexibility in the design of GaAs thin film stress transducers. For the resistors with low linear charge density, the effect of piezoelectric charges dominates the resistance change, as confirmed by the measurements of the resistors oriented along $[01\bar{1}]$ and $[011]$ directions. In addition, an accelerometer is successfully fabricated by micromachining that uses the high etching selectivity between GaInP and GaAs. This high sensitivity of accelerometer originates from the combined effect of low doping as well as the thin beam structure (2.6 μm). Results in this study demonstrate that GaInP/GaAs material system with its piezoelectric modulated effect in n-mesa resistors is highly promising for applications of III–V compound semiconductor smart sensors because its fabrication process is compatible with that of conventional n-channel metal-semiconductor field effect transistor (MESFETs).

ACKNOWLEDGMENT

The authors would like to thank the National Science Council of the Republic of China for financially supporting this research under Contract No. NSC 88-2218-E-002-018.

[1] K. Hjort, J. Söderkvist, and J. Å. Schweitz, J. Micromech. Microeng. **4**, 1 (1994).
[2] K. Fricke, H. L. Hartangel, R. Schütz, G. Schweeger, and J. Würfl, IEEE Trans. Electron Devices **10**, 577 (1989).
[3] K. Fricke, H. L. Hartangel, W. Y. Lee, and J. Würfl, IEEE Trans. Electron Devices **39**, 1977 (1992).
[4] S. J. Harrold, *An Introduction to GaAs IC Design* (Prentice–Hall, Englewood Cliffs, NJ, 1993), p. 7.
[5] W. Kuehnel, and S. Sherman, Sensors and Actuators A **45**, 7 (1994).
[6] Y. Matsumoto, and M. Esashi, Sensors and Actuators A **39**, 209 (1993).
[7] B. Riedel, Analog Dialogue (Analog Devices, Inc., 1993) **27-2**, 3 (1993).
[8] A. Sager, Westinghouse Scientific Paper, 1958 (unpublished), Vol. 8-1038, p. 49.
[9] P. M. Asbeck, C.-P. Lee, and M.-C. F. Chang, IEEE Trans. Electron Devices **31**, 1377 (1984).
[10] Q. A. Huang, Q. Y. Tong, and S. J. Lu, Sens. Actuators A **35**, 247 (1993).
[11] A. Dehé, K. Fricke, K. Mutamba, and H. L. Hartnagel, J. Micromech. Microeng. **5**, 139 (1995).
[12] B. J. Aleck, J. Appl. Mech. **16**, 118 (1949).
[13] R. Zeyfang, Solid-State Electron. **14**, 1035 (1971).
[14] S. Adachi, J. Appl. Phys. **58**, R1 (1985).
[15] H. Booyens, J. S. Vermaak, and G. R. Proto, J. Appl. Phys. **48**, 3008 (1977).
[16] E. J. Charlson and G. Mott, Proc. IEEE **51**, 1239 (1963).
[17] R. S. Muller and J. Conragan, IEEE Trans. Electron Devices **12**, 590 (1965).
[18] T. H. Lim, T. J. Miller, F. Williamson, and M. I. Nathan, Appl. Phys. Lett. **69**, 1599 (1996).
[19] Y. Okamoto, K. Matsunaga, and M. Kuzuhara, IEEE Electron Device Lett. **31**, 2216 (1995).
[20] Y. S. Lin, S. S. Lu, and T. P. Sun, IEEE Electron Device Lett. **16**, 518 (1995).
[21] S. S. Lu and Y. J. Wang, IEEE Electron Device Lett. **15**, 60 (1994).

Downloaded 01 Mar 2009 to 140.112.113.225. Redistribution subject to AIP license or copyright; see http://jap.aip.org/jap/copyright.jsp